Intramolecular Chain Transfer to Polymer in the Emulsion Polymerization of 2-Ethylhexyl Acrylate

Christophe Plessis,[†] Gurutze Arzamendi,[‡] Juan M. Alberdi,[§] Mathias Agnely,[⊥] Jose R. Leiza,[†] and Jose M. Asua*,[†]

Institute for Polymer Materials (POLYMAT) and Grupo de Ingeniería Química, Departamento de Química Aplicada, Facultad de Ciencias Químicas, The University of the Basque Country, Apdo 1072, E-20080 Donostia-San Sebastián, Spain; Departamento de Química Aplicada, Universidad Pública de Navarra, E-31006 Pamplona, Spain; Departamento de Fisica de Materiales, Facultad de Ciencias Químicas, The University of the Basque Country, Apdo 1072, E-20080 Donostia-San Sebastián, Spain; and Rhodia Centre de Recherches d'Aubervilliers, 52 rue de la Haie Coq, F-93308 Aubervilliers Cedex, France

Received October 23, 2000
Revised Manuscript Received May 15, 2001

Introduction

Acrylic polymer latexes are widely used for adhesives, paints, and varnishes. These applications require the formation of a continuous film, and hence the glass transition temperature of the polymer, T_g, should be below room temperature. Polymers having a very low T_g are used for pressure-sensitive adhesives (PSA).[1] Because the polymer becomes softer as the size of the ester group increases, *n*-butyl acrylate (*n*-BA) and 2-ethylhexyl acrylate (2EHA) are basic components of the acrylic latexes.

Plessis et al.[2−7] studied the seeded semicontinuous emulsion polymerization of *n*-BA, finding some remarkable features. Under starved conditions, a highly branched polymer (% branches = 0.9−3.4) containing 50−60% gel was formed. Interestingly, no correlation between branching frequency (measured by solid-state ^{13}C NMR) and gel content was found. The experimental results are well described by the mechanisms outlined in Scheme 1 which includes both intermolecular and intramolecular chain transfer to polymer. These mechanisms can be summarized as follows:

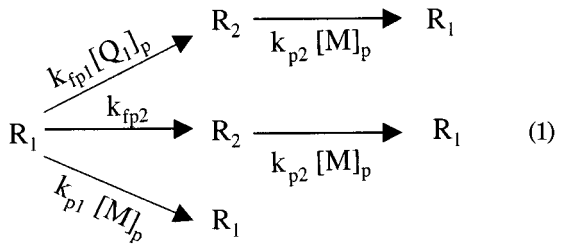

(1)

where R_1 is a secondary carbon radical resulting from propagation reactions and R_2 a tertiary carbon radical formed by chain transfer to polymer. k_{fp1} is the second-order rate constant for the intermolecular chain transfer, $[Q_1]_p$ the concentration of polymer in the polymerization loci (polymer particles), k_{fp2} the first-order rate coefficient for the intramolecular chain transfer to polymer, k_{p1} and k_{p2} the propagation rate constants of radicals R_1 and R_2, respectively, and $[M]_p$ the concentration of monomer in the polymer particles. Mathematical modeling shows that most of the branches are formed by intramolecular chain transfer (backbiting).[4]

Extensive backbiting gives a distinctive kinetic character to the polymerization of *n*-BA as it makes the effective propagation rate constant dependent on monomer and polymer concentrations. According to the reaction paths summarized above, the effective propagation rate constant is

$$\bar{k}_p = k_{p1}P_1 + k_{p2}P_2 \tag{2}$$

where P_1 and P_2 are the probabilities of having a radical of type R_1 and R_2, respectively, given by[4]

$$P_1 = \frac{k_{p2}[M]_p}{k_{p2}[M]_p + k_{fp2} + k_{fp1}[Q_1]_p}; \quad P_2 = 1 - P_1 \tag{3}$$

Because tertiary carbon radicals are much less reactive than secondary radicals[8] ($k_{p2} \ll k_{p1}$), $\bar{k}_p$ decreases as $[M]_p$ decreases. This means that the effective propagation rate constant in emulsion polymerization is substantially lower than that measured by pulsed laser polymerization (PLP/SEC) in bulk.[2]

Scheme 1 has profound technological consequences as it affects both polymerization rate and product properties. Therefore, it is worth checking whether this reaction mechanism applies to other alkyl acrylates. In this work, the applicability of the mechanisms presented above and in Scheme 1 to the emulsion polymerization of 2-ethylhexyl acrylate is investigated. Despite the practical importance of 2EHA, literature about the emulsion polymerization of this monomer is scarce, and the level of branches and the gel content is not reported.[9−11]

Experimental Section

2EHA and acrylic acid (Atochem), sodium hydrogen carbonate (Panreac), and potassium persulfate (Fluka) were used as received. Doubly deionized water was used throughout the work. Seeded semicontinuous polymerizations were carried out in a 1 L glass reactor at 75 °C using a set of three pitch blade impellers at 200 rpm. The recipes for the seed and the semicontinuous experiments are given in Tables 1 and 2. In the semicontinuous process, the seed (d_p = 85 nm, solids content = 20.5 wt %, gel content = 20%, $M_w = 3 \times 10^6$ g/mol and prepared using SLS (Merck)), the surfactant (provided by Rhodia), the initiator, and the water were initially charged into the reactor. The rest of components were fed for 3 h in two streams: a preemulsion of monomer and an initiator solution. The final solids content was about 40 wt %. Samples were withdrawn from the reactor, conversion was measured gravimetrically, and particle size was determined by dynamic light scattering (Coulter N4 Plus) and by capillary hydrodynamic fractionation (CHDF 2000, Matec).[3,17] The sol molecular weight distributions were determined by size exclusion chromatography (SEC) using a dual detector system formed by a differential refractometer and a viscometer. The equipment

[†] Departamento de Química Aplicada, University of the Basque Country.
[‡] Universidad Pública de Navarra.
[§] Departamento de Fisica de Materiales, The University of the Basque Country.
[⊥] Rhodia Centre de Recherches d'Aubervilliers.
* To whom correspondence should be addressed. E-mail: qppasgoj@sq.ehu.es.

10.1021/ma0018190 CCC: $20.00
Published on Web 07/17/2001

Scheme 1

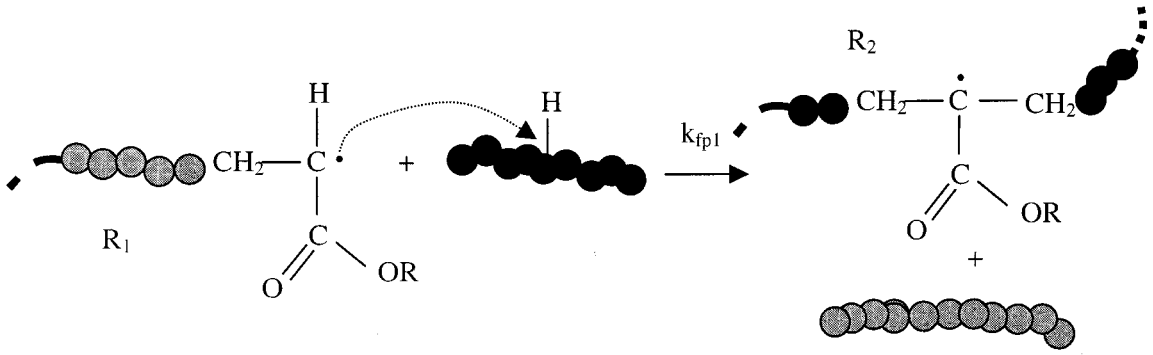

a) Intermolecular chain transfer

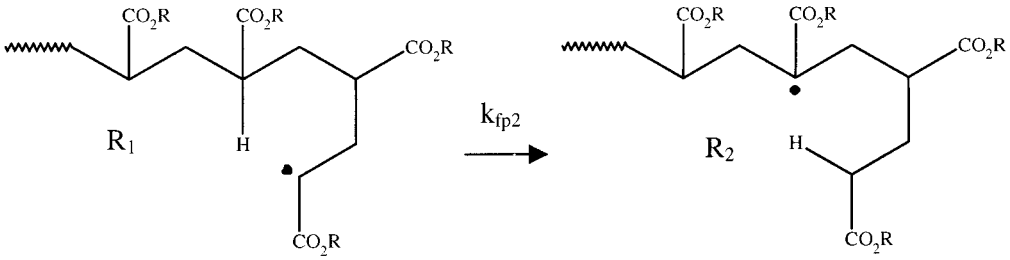

R=n-butyl, 2 ethyl hexyl ...

b) Intramolecular chain transfer

Table 1. Seed Recipe

2-ethylhexyl acrylate (g)	250
water (g)	1000
SLS (g)	5.0
$NaHCO_3$ (g)	1.25
$K_2S_2O_8$ (g)	1.25

Table 2. Recipe Used in the Seeded Semicontinuous Experiments

	initial charge	stream 1	stream 2
polymer[a] (g)	20	–	–
water (g)	97.5[b]	20	255
surfactant A (g)	1.25	–	2.5
2EHA	–	–	225.4
acrylic acid (g)	–	–	4.6
$K_2S_2O_8$ (%)[c]	0.0375 or 0.30		–

[a] Mass of polymer in seed. [b] Mass of water included the water present in the seed. [c] Weight percentage based on the total monomer weight. This amount was the sum of the initial charge plus that added in stream 1. The ratio of initiator between the initial charge and the feed was 1/1.

was calibrated using polystyrene standards, and absolute molecular weights were calculated. The amount of gel was determined by means of an extraction process under reflux conditions in THF. The level of branching was measured by solid-state ^{13}C NMR by analyzing the percentage of quaternary carbons in the spectrum using a calculation method similar to that used for *n*-BA.[2,3,7,11] Figure 1 shows a typical spectrum of poly(2EHA) relevant for this work. Peak assignment is shown in Table 3. The assignments were derived by comparison with hector spectra of the monomer and by comparison of experimental shifts with those calculated using empirical substituent additivity parameters.[12] They were in agreement with data previously published for this monomer.[13] In addition, the DEPT technique was used to determine the multiplicity of the peaks, i.e., whether a given carbon was primary, secondary, tertiary, or quaternary. The mole percent of branched units in the poly(2EHA) samples was calculated as follows:

$$\% \text{ branches} = \frac{A_K}{A_K + \frac{A_{H+J}}{2}} \times 100 \qquad (4)$$

where A_K is the area of the peak corresponding to the quaternary carbon and A_{H+J} the area under peaks corresponding to the CH and CH_2 of the backbone as shown in Figure 1. The sensitivity limit of the quaternary carbon peak is of about 0.4−0.5% branches, and ±15% error can be attributed to the measurement. Additional details for the experimental procedure and the characterization techniques employed in this work can be found elsewhere.[3,7]

Mathematical Model

A mathematical model developed in a previous work[4,7] for *n*-butyl acrylate was used to compare its predictions with the experimental results. The model calculates kinetics, sol molecular weight distribution, MWD, gel fraction, and branching level. Sol MWD and gel were calculated using the numerical fractionation technique developed by Teymour and Campbell[14] as modified by Arzamendi and Asua,[15] and the compartmentalization of the radicals is accounted for by means of the partial distinction concept.[16] Branching was calculated taking

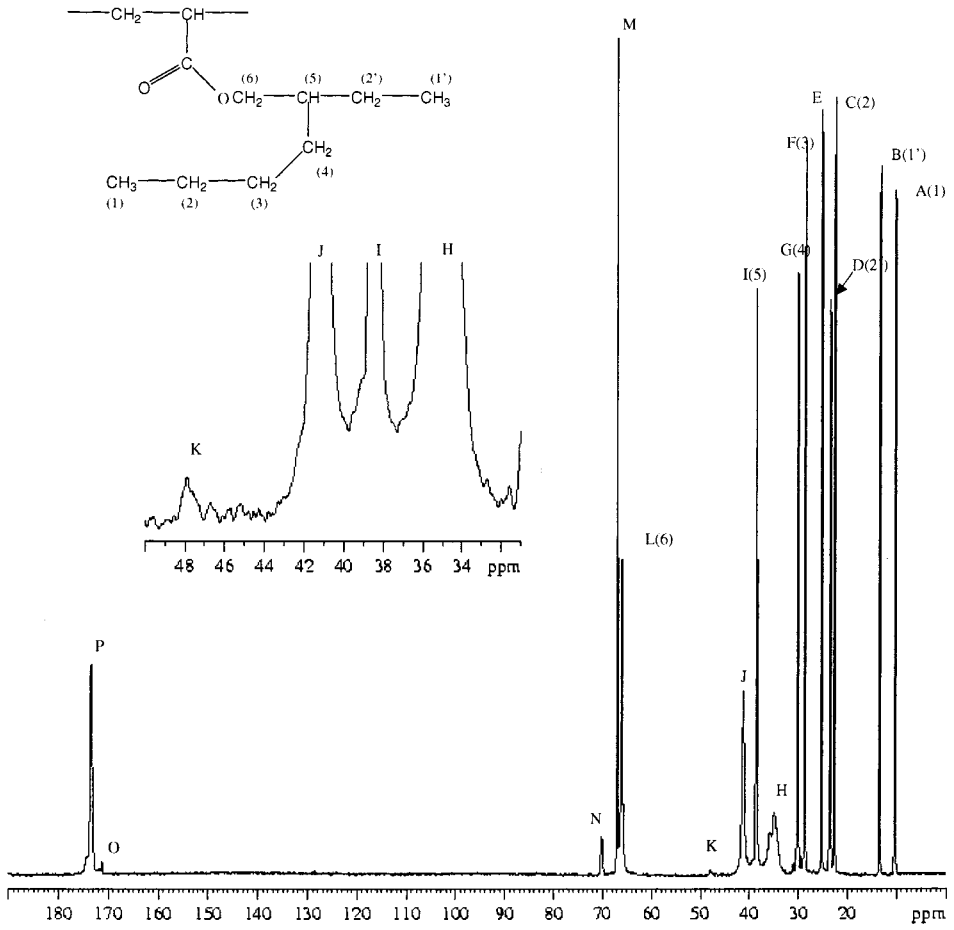

Figure 1. Solid-state ^{13}C NMR spectrum of poly(2-ethylhexyl acrylate) recorded using THF solvent. The assignments of the labeled peaks are given in Table 3.

Table 3. ^{13}C Shift Assignments of 2EHA Polymer

peak	chemical shift (ppm)	carbon
A	10.3	1-CH_3
B	13.4	1′-CH_3
C	22.6	2-CH_2
D	23.5	2′-CH_2
E	25.2	THF
F	28.6	3-CH_2
G	30.1	4-CH_2
H	34.8−35.6	backbone CH_2
I	38.5	5-CH
J	41.2	backbone CH
K	48.0	branch Cq
L	66.0	6-CH_2
M	67.0	THF
N	69.6	surfactant
O	171.2	branch or terminal C=O
P	173.5	2EHA C=O

into account the branches formed by both the intermolecular transfer to polymer and the backbiting mechanism. The latter was modeled as a first-order reaction following the models used for this mechanism for polyethylene.[17] Model parameters (propagation rates and intra- and intermolecular transfer rate constants) were estimated by fitting model predictions to experimental data of sol MWD, gel fraction, branching, and kinetics of two experiments carried out with different initiator concentration. It is worth pointing out that the values of the parameters estimated in this work (Table 5) cannot be taken as definitive values because of the limited number of experiments used for their estimation.

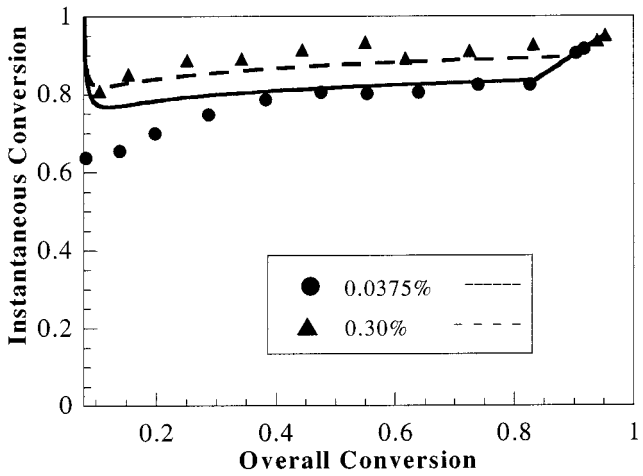

Figure 2. Instantaneous conversion for the latexes prepared with different initiator concentrations. Points correspond to experimental data and lines to model predictions.

Table 4. Experimental and Model Predicted Level of Branches

initiator concentration (wt %)	experimental (%)	model (%)
0.0375	1.4 ± 0.2	1.74
0.3	2.3 ± 0.35	2.35

Results and Discussion

Figure 2 presents the evolution of the instantaneous conversion and Table 4 the percentage of branches of the final latexes for two initiator concentrations. It can

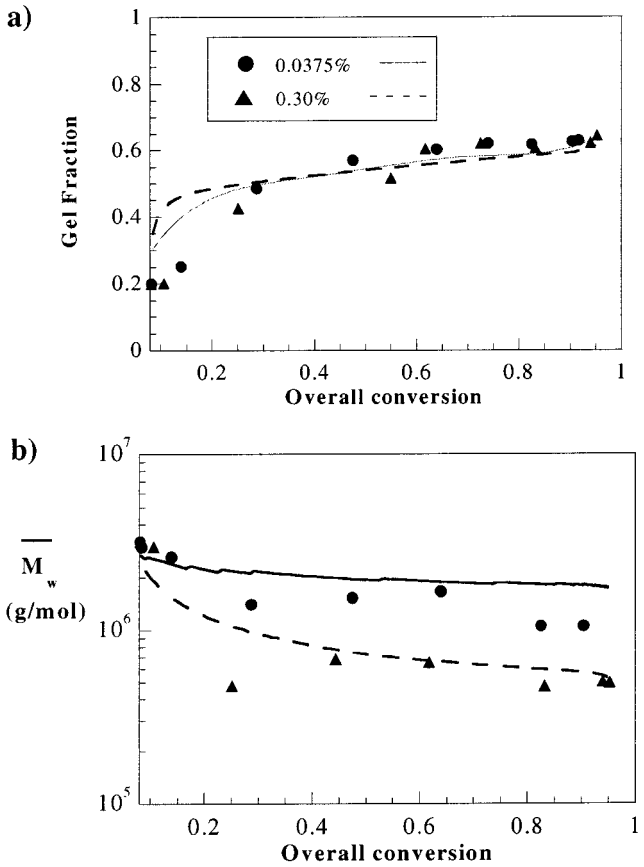

Figure 3. Fraction of gel (a) and weight-average molecular weight (b) for the latexes prepared with different initiator concentrations. Points correspond to experimental data and lines to model predictions.

be observed that conversion increased with initiator concentration. This increase was due to an increase of the average number of radicals per particle because the number of polymer particles was not affected by the initiator concentration (not shown). On the other hand, the level of branches increased when increasing the initiator concentration (Table 4).

Figure 3 shows the effect of initiator concentration on both the weight-average molecular weight of the sol polymer and the gel content. The fraction of gel increases from 20% (corresponding to the gel content of the seed) to 60−65 wt % (Figure 3a). The final gel content was not affected by the initiator concentration. Figure 3b shows that $\bar{M}_w$ decreased along the process. Most of the decrease correspond to the first part of the reaction. Besides, the lower the initiator concentration, the higher the sol molecular weight.

The results shown in Figures 2 and 3 present similar features to those obtained in the emulsion polymerization of *n*-BA.[2,3] This strongly suggests that the emulsion polymerization of 2EHA also proceeds according to the mechanism presented above. The results presented in Figures 2 and 3 were analyzed by means of a mathematical model that included the calculation of branching, gel fraction, and sol molecular weight distribution.[4] Model predictions are shown in Figures 2 and 3 and the estimated model parameters in Table 5. It can be seen that the model predicts reasonably well all the experimental data. According to the model, the initiator concentration affected the polymerization rate in two ways. First through the average number of radicals per particle, $\bar{n}$, that increased with the initiator concentration ($\bar{n}$ is the range 0.3−0.5 and 0.5−1.2 for 0.0375 and 0.3 wt % of initiator, respectively). Second, the variation in $\bar{n}$ affected the monomer conversion, i.e., the concentrations of monomer and polymer in the polymer particles, which in turn modified the effective propagation rate constant (eqs 2 and 3). Figure 4 shows the effective propagation rate constant calculated by the model with the estimated values of the parameters (Table 5). It can be seen that $\bar{k}_p$ decreased as monomer concentration decreased. Note that the dependence of $\bar{k}_p$ in $[M]_p$ appeared as linear because $k_{fp2} \gg k_{p2}[M]_p \gg k_{fp1}[Q_1]_p$ in this case. Conflicting results on the effect of monomer concentration on the effective propagation rate constant of acrylic monomers have been reported. Plessis et al.[3,4] found that $\bar{k}_p$ increased with monomer concentration in the emulsion polymerization of *n*-BA. On the other hand, for the bulk polymerization of *n*-BA, Buback and Degener[19] using excimer laser techniques in conjunction with time-resolved high-pressure near-infrared spectroscopy reported that $k_p\phi_i$ (ϕ_i being the quantum yield) remained constant up to about 80% conversion. The authors assumed that ϕ_i was constant, and hence k_p was independent of monomer concentration. The main drawback of this work is that only conversion data were used to estimate k_p, ϕ_i, and k_t, obtaining a value of k_p at 25 °C (k_p = 3168 L/(mol s)) several times smaller than that measured by PLP/SEC ($k_p \cong$ 15 500 L/(mol s)).[20,21]

Another conflicting point is the effect of the length of the ester group on k_p. Beuerman et al.[21] reported that the propagation rate constant increased with the length of the ester group in the range 5−25 °C. On the other hand, Capek et al.[9] and Samer and Schork[10] found that the polymerization of 2EHA was slower than that of *n*-BA. The results obtained in the present work are in agreement with the findings of Capek et al.[9] and Samer

Table 5. Values of Parameters Used for the Model Predictions in Figures 2−4

parameters	R_1	R_2
k_p (L/(mol s))	5.68×10^4 [b]	34[b]
k_{to} (L/(mol s))	6×10^6 [4]	6×10^6 [4]
k_{fp1} (L/(mol s))	0.530[b]	0.230[b]
k_{fp2} (s^{-1})	920[4]	−
$C_{tr,M} = k_{tr,M}/k_p$	8.8×10^{-5} [18]	8.8×10^{-5} [18]
a_1[a]	2.49 [4]	2.49 [4]
k_a* (dm^2/(mol s))[a]	4.2×10^{-9} [4]	8.1×10^{-9}
k_d* (dm^2/s)[a]	4.5×10^{-11} [4]	

[a] $k_t = k_{t0} \exp(-a_1\Phi_p^p)$; $k_d = k_d^*/r_p$; $k_a = k_a^* r_p$. [b] Estimated parameters.

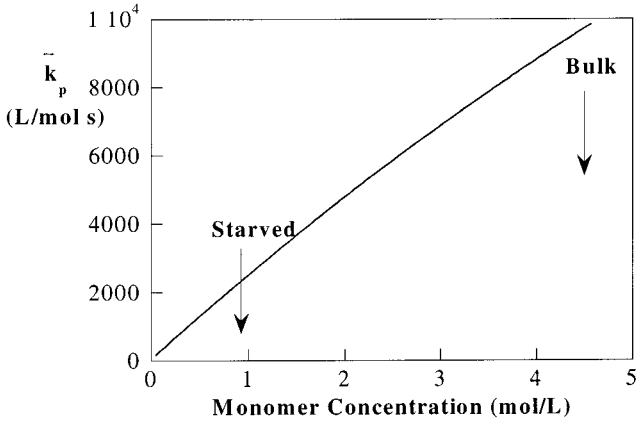

Figure 4. Effect of monomer concentration on the effective propagation rate constant of 2EHA at 75 °C.

and Schork[10] because the polymerization rate in the experiments reported in this work is clearly lower than that measured in experiments conducted with *n*-BA[2] at the same conditions. The estimated value of k_{p1} for 2EHA (56 800 L/(mol s)) is slightly larger than that found for *n*-BA[2] (53 460 L/(mol s)). However, when the effective propagation rate constants at 75 °C for bulk polymerization are calculated (using eqs 2 and 3 with [2EHA] = 4.5 mol/L; [*n*-BuA] = 6.5 mol/L and the values of the parameters in Table 5 and ref 2), the effective propagation rate constant of 2EHA (k_{pbulk} = 9713 L/(mol s)) was found to be smaller than that of the *n*-BA(k_{pbulk} = 22 292 L/(mol s)). This result explains the fact that the polymerization rate of 2EHA is lower than that of *n*-BA. However, the value of the effective k_p calculated in bulk at 75 °C for 2EHA (9713 L/(mol s)) was smaller than the value calculated by extrapolation of Beuermann et al.[21] data (30 700 L/(mol s)). This was not the case for *n*-BA in which the effective k_p value calculated for bulk conditions compared well with the value extrapolated at 75 °C from PLP/SEC data of Beuermann et al.[20] Admitedly, no reason for the discrepancy in the k_p value for 2EHA under bulk conditions can be offered. Nevertheless, it is worth pointing out that this comparison is the result of two extrapolations: (i) that of the $\bar{k}_p$ estimated in this work to bulk conditions and (ii) that of the Beuermann's k_p from 25 to 75 °C. In addition, it should be noted that the parameters estimated in this work are only obtained from two experiments, and hence they should be regarded as a rough estimation. The experimental data reported in the present work could not be fitted by using Beuermann's effective k_p.

Table 4 shows that in agreement with the experimental results the level of branches predicted by the model increased with the initiator concentration. Actually, branching increased with monomer conversion (that increased with initiator concentration) because according to the presented mechanism, the lower the monomer concentration, the more likely the intramolecular chain transfer to polymer. According to the model, backbiting was the predominant branching mechanism; namely, most of branches were short-chain branches. Nevertheless, it is worth noting that although the number of long chain branches formed by intermolecular transfer to polymer was significantly lower than the short-chain branches formed by backbiting, the former definitely contributed to the formation of gel; namely, that without those branches no gel could be produced.

Figure 3 shows that the model predicts reasonable well the evolution of gel content and molecular weights. According to the model, the decrease of $\bar{M}_w$ with the initiator concentration was the result of two effects. First, as the initiator concentration increased, the entry rate increased, inducing an increase of the termination rate and a decrease of the average lifetime of the growing chains. Second, the increase of initiator concentration made the process proceeded under more starved conditions which increased intermolecular chain transfer to polymer. The incorporation of long chains to the gel was also responsible for the decrease of $\bar{M}_w$ along the process.

Chiefari et al.[22] reported that polymer chain fragmentation by β-scission may occur in acrylic polymers after formation of tertiary radicals by chain transfer to polymers. β-Scission increased as temperature increased and monomer concentration decreased. The lowest temperature at which significant polymer chain fragmentation by β-scission was reported was 80 °C, and this required a very low monomer concentration (15 wt %). No evidence of polymer chain fragmentation by β-scission was found in the present work, likely due to the low temperature (75 °C) and relatively high monomer concentrations (10−35 wt %) used.

Conclusions

In the foregoing it has been shown that the emulsion polymerization of 2EHA presents similarities to the polymerization of *n*-BA. This allowed to demonstrate that the reaction scheme proposed for *n*-BA was also operative for 2EHA. This scheme involves both secondary and tertiary carbon radicals. Secondary radicals are produced by propagation reactions, and the tertiary radicals result from chain transfer to polymer, mostly from backbiting. The tertiary radicals are less reactive than the secondary ones, and hence extensive backbiting yields a lower effective propagation rate constant. A consequence of this reaction scheme is that the effective propagation rate constant depends on the monomer and polymer concentrations in the polymerization loci. The effective propagation rate constant extrapolated to bulk conditions differed from that estimated by extrapolation of Beuermann's[21] data from 25 to 75 °C.

Acknowledgment. The financial support by the Diputación Foral de Gipuzkoa and the University of the Basque Country is greatly appreciated.

Nomenclature

a_1 = parameter for the gel effect relationship
k_a = entry rate coefficient (L/(mol s))
k_d = desorption rate coefficient (s^{-1})
k_{fp1} = intermolecular chain transfer to polymer rate constant (L/(mol s))
k_{fp2} = rate constant for backbiting (s^{-1})
k_p = propagation rate constant (L/(mol s))
k_{t0} = rate constant for termination by combination rate constant at zero conversion (L/(mol s))
$k_{tr,M}$ = monomer chain transfer rate constant (L/(mol s))
R_1 = secondary radical generated by propagation
R_2 = tertiary radical generated by backbiting of R_1

References and Notes

(1) De Fusco, A. J.; Sehgal, K. C.; Basset, D. R. In *Polymeric Dispersions: Principles and Applications*; Asua, J. M., Ed.; Kluwer Academic Publishers: Dordrecht, 1997; p 379.
(2) Plessis, C.; Arzamendi, G.; Leiza, J. R.; Schoonbrood, H. A. S.; Asua, J. M. *Macromolecules* **2000**, *33*, 4.
(3) Plessis, C.; Arzamendi, G.; Leiza, J. R.; Schoonbrood, H. A. S.; Asua, J. M. *Macromolecules* **2000**, *33*, 5041.
(4) Plessis, C.; Arzamendi, G.; Leiza, J. R.; Schoonbrood, H. A. S.; Charmot, D.; Asua, J. M. *Ind. Eng. Chem. Res.*, in press.
(5) Plessis, C.; Arzamendi, G.; Alberdi, J. M.; Leiza, J. R.; Schoonbrood, H. A. S.; Asua J. M. *J. Polym. Sci., Part A: Polym. Chem.* **2001**, *39*, 1106.
(6) Plessis, C.; Arzamendi, G.; Leiza, J. R.; Schoonbrood, H. A. S.; Charmot, D.; Asua, J. M. *Macromolecules* **2001**, *34*, 5147.
(7) Plessis, C. Ph.D. Dissertation, The University of the Basque Country, Donostia-San Sebastián, 2001.
(8) Mcord, E. F.; Shaw, W. H.; Hutchinson, R. A. *Macromolecules* **1997**, *30*, 246.
(9) Capek, I.; Juranicova, V.; Barton, J.; Asua, J. M.; Ito, K. *Polym. Int.* **1997**, *43*, 1.
(10) Samer, C. J.; Schork, F. J. *Ind. Eng. Chem. Res.* **1999**, *38*, 1792.
(11) Ahmad, N. M.; Heatley, F.; Lovell, P. A. *Macromolecules* **1998**, *31*, 2822.

(12) Pretsch, E.; Clerc, T.: Seibl, J.; Simon, W. In *Tablas para la elucidación estructural de compuestos orgánicos por métodos espectroscopios*; Alhambra: Madrid, 1980.
(13) Vlcek, P.; Kriz, J. *J. Polym. Sci., Part A: Polym. Chem.* **1992**, *30*, 1511.
(14) Teymour, F.; Campbell, J. D. *Macromolecules* **1994**, *27*, 2460.
(15) Arzamendi, G.; Asua, J. M. *Macromolecules* **1995**, *28*, 7479.
(16) Arzamendi, G.; Sayer, C.; Zoco, N.; Asua, J. M. *Polym. React. Eng.* **1998**, *6*, 193.
(17) Kiparissides, C.; Verros, G.; McGregor, J. F. *J. Macromol. Sci., Rev. Macromol. Chem. Phys.* **1993**, *C33* (4), 437.
(18) Maeder, S.; Gilbert, R. G. *Macromolecules* **1998**, *31*, 4410.
(19) Buback, M.; Degener, B. *Makromol. Chem.* **1993**, *194*, 2875.
(20) Lyons, R. A.; Hutovic, J.; Piton, M. C.; Christie, D. I.; Clay, P. A.; Mander, B. G.; Kable, S. H.; Gilbert, R. G. *Macromolecules* **1996**, *29*, 1918.
(21) Beuermann, S.; Paquet, D. A.; McMinn, J. H.; Hutchinson, R. A. *Macromolecules* **1996**, *29*, 4206.
(22) Chiefari, J.; Jeffery, J.; Mayadunne, R. T. A.; Moad, G.; Rizzardo, E.; Thang, S. H. *Macromolecules* **1999**, *32*, 7700.

MA0018190